Image Analysis in Dual Modality Tomography for Material Classification

I. Basarab-Horwath[1], A. T. Daniels, R. G. Green
School of Engineering, Sheffield Hallam University,
City Campus, Sheffield, S1 1WB.

Abstract

A dual modality tomographic system is described for material classification in a simulated multi-component flow regime. It combines two tomographic modalities, electrical current and light, to image the interrogated area. Derived image parameters did not allow material classification. PCA analysis was performed on this data set producing a new parameter set, which allowed material classification. This procedure reduces the dimensionality of the data set and also offers a pre-processing technique prior to analysis by another classifier.

Introduction

Dual-modality tomography is a technique that uses two modalities to produce two separate tomographic images of the same interrogated area or object. Since, in principle, each modality produces a mapping or image of the distribution of separate or different object properties, dual-modality tomography produces two (complimentary) images of an object which show the distribution of two separate object properties. This paper describes preliminary work that demonstrates that it is possible to combine the output from these two modalities to enable classification of the materials flowing through that interrogated area.

There is also an increasing amount of work into spectroscopic methods. These are best classed as quasi-multi-modal systems; only one modality is used but at different excitation modes in order to differentiate between the various components within an object or interrogated area. Multi-spectral work has been used in remote sensing, medicine and process tomography [1, 2, 3]. One rather interesting application of this type of work is the use of a range or spectrum of X-ray energies, along with principal component analysis (PCA), to identify materials in baggage handling [4]. Relatively little work has been carried out on multi-modal tomography [5, 6, 7, 8, 9] and as such it is difficult to comment on exactly which is the better method for material classification. In principal, dual modality tomography should allow classification without the need to characterise each material over a spectrum of excitations for a single modality. However, there are situations where only one modality can be easily applied – e.g. electrical impedance tomography (EIT) in medical/physiological measurements - and hence spectroscopic techniques have a larger role in these applications.

An example of multi-component flow is the flow of materials in sewers. Typically, the materials flowing in sewers, in addition to water, are perspex, plastic, gas bubbles, rubber products and paper. These materials cannot be distinguished from one another using a single modality other than to determine whether they are good or bad electrical conductors or to determine the degree to which they allow light to pass through them. Thus material identification cannot be carried out with a single modality in such an environment although it is possible to perform rather crude classification. Dual-modality tomography should, given a suitable choice of modalities, permit the classification of these materials.

Method

The materials chosen for this experimental work were perspex, opaque plastic, paper and rubber [10]. Because the objective of this work was only to demonstrate the principal of dual modality tomography, the experimental work was carried out in a tank with no movement of the materials. The materials were in the form of cylinders; a bubble was simulated using an acetate sheet rolled into a cylinder of the appropriate dimensions and sealed at both ends. The normalised radius of each cylinder of material relative to the radius of the tank was 0.25, i.e. a normalised area of 0.0625. Measurements were also

[1] Please address all correspondence to Dr. I. Basarab-Horwath.

made on combinations of these materials - three combinations were chosen: rubber and paper, perspex and rubber and also perspex and paper. There was therefore a total of eight different materials or combinations of materials and therefore eight measurements or images for each modality, giving a total of sixteen images.

The two modalities chosen to interrogate a 'model' pipeline or phantom were electrical current to determine the electrical impedance distribution within the pipe and infra-red (IR) to determine the 'optical' transmission distribution or IR opacity. The electrical impedance system used was a standard adjacent-pair sixteen electrode system operating at 8 kHz. The IR system consisted of two arrays of eight LEDs, positioned so as to be mutually orthogonal to each other and to the central axis of the pipe. The experimental arrangement illustrated in Figure 1 shows a side view of phantom and a plan view of half the cross-section viewed along the vertical axis of the phantom, both figures show the position of the electrodes and IR sensors.

Images of the distribution of electrical impedance were produced using a back-projection algorithm [11]. Similarly, images of the IR transmittance distribution were constructed using a sensitivity coefficient algorithm [12]. The IR image can be used to accurately place the object or objects in the pipeline in one or more of 64 square pixels. The images cannot be combined sensibly using logical or arithmetic functions [10]. One particular method is to treat corresponding pixel values from the two images as elements in a 2D vector, that is, as if the electrical and IR images were orthogonal to each other. In fact, each material and material combination did produce its own unique scatter diagram. Unfortunately, material combinations did not have a scatter plot that was a combination of the scatter plots of the separate materials. Thus cluster analysis could be applied to the dual modality scatter plots of individual materials but not to combinations of materials. Also, it was clear that a scatter plot of a material combination was not a convolution or cross-correlation of the scatter plots of the individual materials. These effects are due to the non-linearity of a soft modality such as EIT, where the image is not material independent, that is, not independent of the resistance distribution. Thus the statistics chosen to analyse the images had to be material invariant. The method chosen to analyse the images was to first construct the histogram of grey scale amplitudes for both images and then to perform an analysis on these histograms [1]. Seven measures were calculated for each of the histograms from the two images; the mean, variance, dispersion, mean square value (or energy), skewness, kurtosis and median. There was therefore a total of fourteen measures representing the two images for every one of the eight materials. Again, there was little correlation in terms of material properties between any of these measures. One method used to look at possible correlations between the measures was to plot each of the seven measures for each image (a total of eight sets of fourteen numbers; one set for each material) against the corresponding values of another measure. There appeared to be no material classification taking place.

Theoretical background

A set of uncorrelated variables that can describe the images better can be obtained from the original set of measures using principal component analysis (PCA). PCA transforms a data set of several correlated measurements for each of several individuals or objects into a set of uncorrelated variables. In most cases the effect is to reduce the dimensionality of a problem and to bring out structure in the data [13, 14]. PCA has also been used to look at tomographic images from mixing vessels and this has been correlated with impeller speeds with a view to adjusting impeller speeds [15, 16]. In the work described here the eight sets (one for each material combination) of fourteen variables (seven variables per image) used to describe the sixteen images are replaced, after PCA, with a smaller number of variables that are uncorrelated. Ideally it is desirable to only have two or three resulting variables since the relationship between these new variables is then relatively easy to understand graphically.

The singular value decomposition of the data matrix D gives $D=URV^T$, where U and V are both column-orthogonal matrices and R is a (square) diagonal matrix of singular values [17] of the data matrix. The normalised transformed data is given by [14]

$$B = \frac{1}{R} U^T D = V^T$$

where B here is an 8 by 8 matrix, each row being the transformed data for a particular material or combination of materials. The amount of information contained in each column (element) is related to the magnitude of the corresponding (diagonal) element in the matrix R since the variance in the data 'explained' by any eigenvector is proportional to the root of the corresponding eigenvalue. The eigenvector associated with the largest eigenvalue accounts for the maximum variance in the data in a least square sense and so on in a decreasing fashion for decreasing values of eigenvalue.

Results

The results of the analysis were stored in the B matrix. The first four eigenvalues, from the R matrix, were 2.43, 1.38, 1.09, 0.74 and continued to decay virtually exponentially. However, it was interesting to note that column B_1, the first column in the B matrix and which corresponds to the largest eigenvalue, does not allow sorting or classification of the materials. Combinations of other columns did however allow classification. Figure 2 shows a plot of the 3rd and 4th columns of the B matrix, referred to as B_3 and B_4. These columns correspond to the 3rd and 4th largest eigenvalues of the C matrix. It can be seen in this projection that there is classification in the B_3, B_4 plane. Plastic and rubber (opaque, non-conducting) lie in the $B_3<0$, $B_4<0$ quadrant while perspex and the bubble lie in the $B_4<0$, $B_3>0$ quadrant (transparent, non-conducting). Paper is virtually on the $B_4=0$ line ($B_3 \approx 0$). Interestingly, paper will absorb water and becomes weakly conducting and partially transparent. The $B_3<0$, $B_4>0$ quadrant contains the combinations of perspex/paper and rubber/paper while the perspex/rubber combination is located in the $B_3>0$, $B_4>0$ quadrant. It is important to note that these classifications or groupings are not apparent in the raw data. Figure 3 shows the B_2 and B_4 columns plotted against each other. Here again, it can be seen that the materials have been classified, albeit with a different classification from that in the B_3, B_4 plane.

Discussion and Conclusions

This analysis technique has shown that there are some data invariant statistics present in the images produced by a ‘simple’ back-projection algorithm. This method of analysis is able to produce classification - but it has to be shown that these are the same co-ordinates for the same material in each experiment. Although the hard field modalities will produce the same local image for each embedded object within the interrogated area this cannot be true by definition for the soft field modalities. This makes PCA sensitive to the details of the data. There may well be image parameters that are only material dependent but not 'soft-field' dependant. Unfortunately, PCA is not image invariant and will thus produce a different set of results for the same materials if the materials are distributed differently within the interrogated area, i.e. the images are different. However, there is also a problem in that if each material were represented by a direction in space one would expect combinations of materials to lie between the pure materials. For example, given a direction for rubber and another for paper then one would expect a rubber/paper combination to lie on or close to the plane joining them. It is interesting to note from these results that this is not the case. However, it has been shown in this work that a factor analysis technique such as PCA performed on image-derived data reduces the dimensionality of the data set and can be used as a crude classifier of materials. What these results do indicate is that the classifier statistics are not, counter-intuitively, some linear combination of the basic image parameters, that is, resistivity/conductivity or IR transparency/opacity. These results also show that this method of analysis can also be used as a pre-processing technique prior to analysis by some other classifier, such as neural networks - the results presented here are linearly separable and as such are amenable to analysis by relatively simple nets.

Acknowledgements

IBH would like to thank Professor D. Barber, University of Sheffield, for invaluable advice as well as Professor B. W. Jervis and Drs. K. Dutton and R. McLaughlin, Sheffield Hallam University, for useful discussions.

References

[1] Jain, A K, Fundamentals of Digital Image Processing, Prentice-Hall, 1989, ISBN 0-13-336165-9
[2] Brown, B H Barber, D C, Wei Wang, Liqin Lu, Leathard, A D, Smallwood, R H, Hampshire, A R, Mackay, R, Hatzigalanis, K, Multi-frequency imaging and modelling of respiratory related electrical impedance changes, Physiol. Meas., 15, Suppl. 2A, A1-A12, May, 1994
[3] Barlow, R K, Williams, R A, Bond, J, Oliver, K T, Hunt, P, Composition analysis of mixed mineral suspensions using impedance spectroscopy, pp 131-136, Frontiers in Industrial Process Tomography 2, April 8-12, 1997, Tech. Univ. Delft, Nederlands.
[4] Maitrejean, S, Perion, D, Sundermann, D, Non-destructive chemical identification using an x-ray transmission function obtained with the multi-energy method, SPIE Conf. Hard X-Ray and Gamma-Ray Detector Physics and Applications, San Diego, California, July, 1998, SPIE Vol. 3446, pp 134-152.
[5]Johansen, G A, Multi-sensor tomography, in 'Process Tomography - 1995, Implementation for industrial processes', Proceedings of a Workshop held in Bergen, 6-8 April 1995, Eds. Beck, M S et al, ISBN 0 9523165 2 8.
[6] Johansen, G A, Froystein, T, Hjertaker, B T, Olsen, O, A dual sensor flow imaging tomographic system, Meas. Sci. Tech., 7, 3, 297-307, pp March, 1996.
[7] Hjertaker, B T, Static characterisation of a dual sensor flow imaging tomographic system, p 53, Frontiers in Industrial Process Tomography 2, April 8-12, 1997, Tech. Univ. Delft, Nederlands.
[8] Schwartz, A, Multi-tomographic flame analysis with a schlieren apparatus, Meas. Sci. Tech., 7, 3, 406-413, pp March, 1996
[9] West, R M, Williams R A, Opportunities for Data Fusion in Multi-Modality Tomography, Proc. 1st World Congress on Industrial Process Tomography, Buxton, Greater Manchester 14–17 April 1999, pp 195 – 200
[10] Daniels, A R, An Investigation into the use of dual modality tomography for the monitoring of constituent volumes in multi-component flows, PhD thesis, Sheffield Hallam University, 1995.
[11] Gadd R, Record P, Rolfe P, A sensitivity region reconstruction algorithm using adjacent drive current injection strategy, Clin. Phys. Physiol. Meas., 13, Suppl. A, pp 101-5, 1992.
[12] Dugdale, W P, An optical instrumentation system for the imaging of two component flows, PhD thesis, Bolton Institute of Higher Education, 1994.
[13] Hotelling, H, Analysis of a complex of statistical variables into principal components, J. Educational Psychology, 24, September, pp 417- 441 and October, pp 498 – 520, 1933.
[14] Martel, Anne L, The use of factor methods in the analysis of dynamic radionuclide studies, PhD thesis, University of Sheffield, June 1992.
[15] Ni, X, Simons, S J R, Williams, R A, Jia, X, Use of PCA and neural networks to extract information from tomographic images for process control, pp 309-314, Frontiers in Industrial Process Tomography 2, April 8-12, 1997, Tech. Univ. Delft, Nederlands.
[16] Tabe H, Simons S J R, Savery, J, West, R M, Williams, R A, Modelling of Multiphase Processes Using Tomographic Data for Optimisation and Control, Proc. 1st World Congress on Industrial Process Tomography, Buxton, Greater Manchester, April 14-17, 1999.
[17] Press W H, Teukolsky S A, Vetterling W T, Flannery B P, Numerical Recipes, CUP, 1992, 2nd Edition, ISBN 0 521 43064 X.

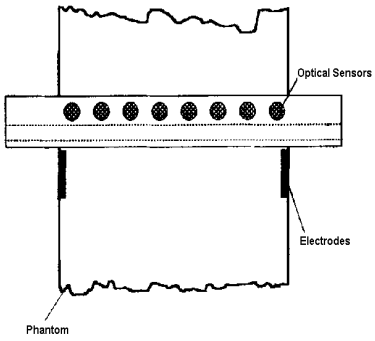

(a)

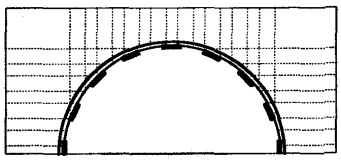

(b)

Figure 1: (a) Side view of phantom and (b) plan view of half the cross-section viewed along the vertical axis of the phantom, both showing the position of the electrodes and IR sensors.

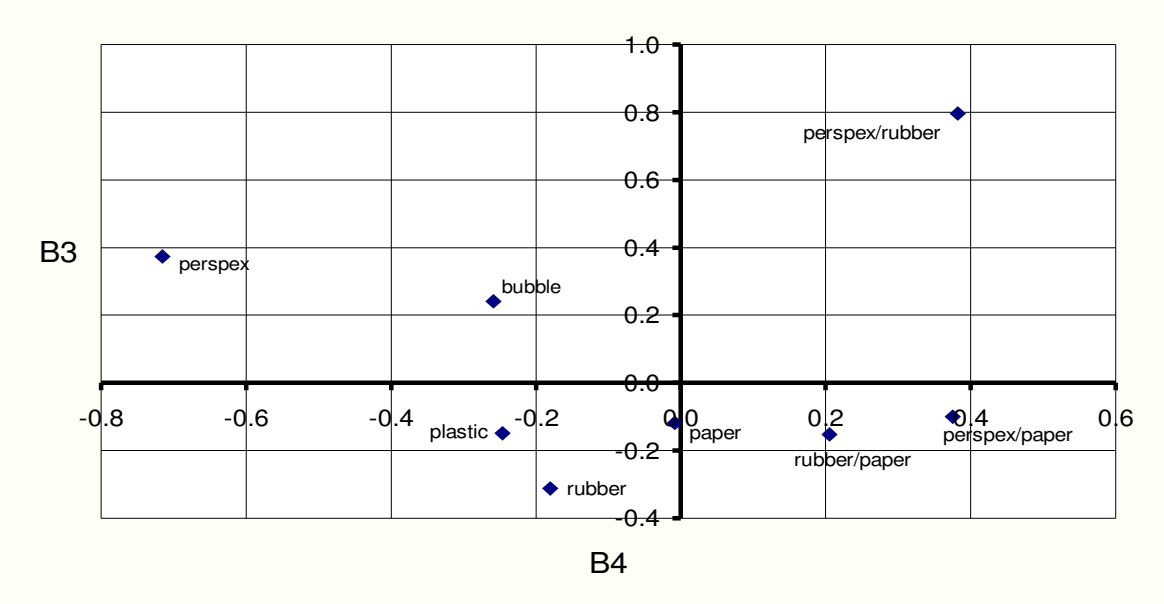

Figure 2. Plot of the two principal components B3 and B4 for each of the eight material combinations.

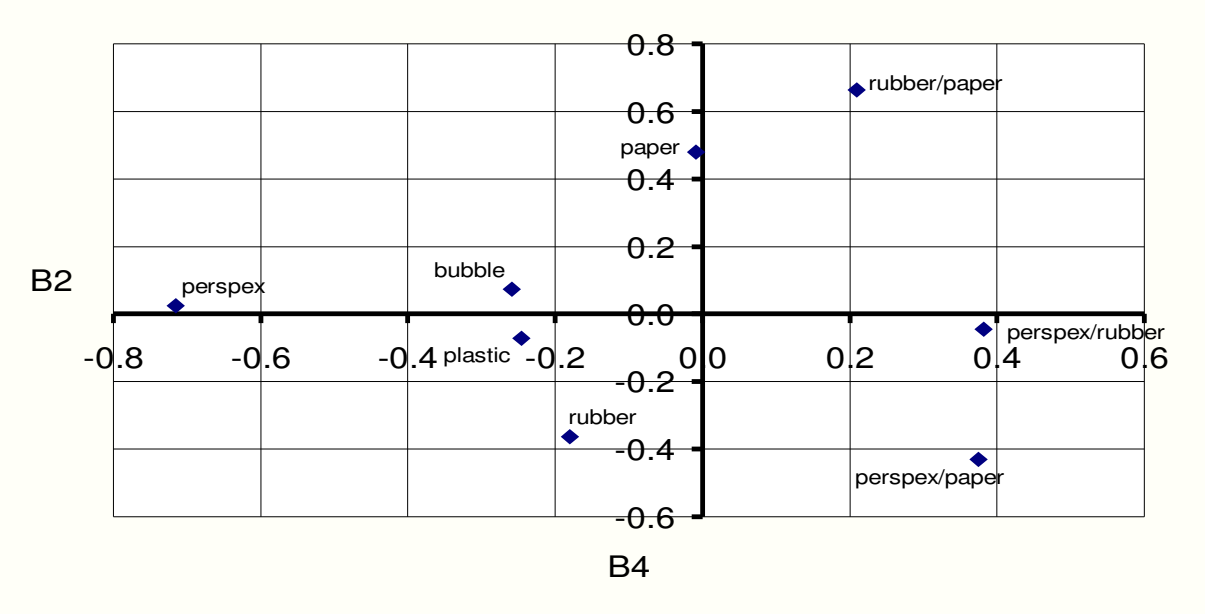

Figure 3. Plot of the two principal components B2 and B4 for each of the eight material combinations.